PNAS Nexus, 2024, 3, pgae452
https://doi.org/10.1093/pnasnexus/pgae452
Advance access publication 9 October 2024
Research Report

The fully activated open state of KCNQ1 controls the cardiac "fight-or-flight" response

Panpan Hou[a,*,1], Lu Zhao[a], Ling Zhong[a], Jingyi Shi[a], Hong Zhan Wang[b], Junyuan Gao[b], Huilin Liu[b], Joan Zuckerman[b], Ira S. Cohen[b] and Jianmin Cui[a,*]

[a]Department of Biomedical Engineering, Center for the Investigation of Membrane Excitability Disorders, Washington University, St. Louis, MO 63130, USA
[b]Department of Physiology and Biophysics, Institute for Molecular Cardiology, Stony Brook University, Stony Brook, NY 11794, USA
[1]Present address: Dr. Neher's Biophysics Laboratory for Innovative Drug Discovery, State Key Laboratory of Quality Research in Chinese Medicine, Macau University of Science and Technology, Taipa, Macao SAR, China.
*To whom correspondence should be addressed: Email: jcui@wustl.edu (J.C.); Email: pphou@must.edu.mo (P.H.)
Edited By: J. Silvio Gutkind

Abstract

The cardiac KCNQ1 + KCNE1 (I_{Ks}) channel regulates heart rhythm under both normal and stress conditions. Under stress, the β-adrenergic stimulation elevates the intracellular cyclic adenosine monophosphate (cAMP) level, leading to KCNQ1 phosphorylation by protein kinase A and increased I_{Ks}, which shortens action potentials to adapt to accelerated heart rate. An impaired response to the β-adrenergic stimulation due to KCNQ1 mutations is associated with the occurrence of a lethal congenital long QT syndrome (type 1, also known as LQT1). However, the underlying mechanism of β-adrenergic stimulation of I_{Ks} remains unclear, impeding the development of new therapeutics. Here, we find that the unique properties of KCNQ1 channel gating with two distinct open states are key to this mechanism. KCNQ1's fully activated open (AO) state is more sensitive to cAMP than its intermediate open state. By enhancing the AO state occupancy, the small molecules ML277 and C28 are found to effectively enhance the cAMP sensitivity of the KCNQ1 channel, independent of KCNE1 association. This finding of enhancing AO state occupancy leads to a potential novel strategy to rescue the response of I_{Ks} to β-adrenergic stimulation in LQT1 mutants. The success of this approach is demonstrated in cardiac myocytes and also in a high-risk LQT1 mutation. In conclusion, the present study not only uncovers the key role of the AO state in I_{Ks} channel phosphorylation, but also provides a target for antiarrhythmic strategy.

Keywords: I_{Ks} channel, phosphorylation, "fight-or-fight" response, long QT syndrome, antiarrhythmia

Significance Statement

The increase of I_{Ks} potassium currents with adrenalin stimulation is important for "fight-or-flight" responses. Mutations of the I_{Ks} channel reducing adrenalin responses are associated with more lethal form of the type-1 long QT syndrome (LQT). The alpha subunit of the I_{Ks} channel, KCNQ1 opens in two distinct open states, namely the intermediate open (IO) and activated open (AO) states, following a two-step voltage-sensing domain activation process. We found that the AO state, but not the IO state, is responsible for the adrenalin response. Modulators that specifically enhance the AO state occupancy can enhance adrenalin responses of the WT and LQT-associated mutant channels. These results reveal a mechanism of state-dependent modulation of ion channels and provide an antiarrhythmic strategy.

Introduction

In the heart, the voltage-gated KCNQ1 potassium channel associates with its KCNE1 modulatory subunit to form the slowly activating delayed rectifier I_{Ks} (KCNQ1 + KCNE1) channel, which contributes to the repolarization of cardiac action potentials (APs) (1). Congenital mutations in both *KCNQ1* and *KCNE1* genes can cause long QT syndrome (LQTS), which shows a prolongation of the QT wave interval in a patient's electrocardiogram and a propensity to ventricular tachyarrhythmias that may lead to cardiac arrest and sudden death (2–5). LQTS is associated with variants of various ion channels and other proteins (6), but LQTS type 1 (LQT1) is due to loss-of-function mutations in KCNQ1 and is the most common congenital LQTS, accounting for more than one-third of all cases (7, 8).

I_{Ks} plays a key role in controlling the heart rhythm, especially under stress conditions that require increased cardiac output following the β-adrenergic stimulation. This process is also known as the cardiac adaptation (or the "fight-or-flight" response), during

Competing Interest: J.S. and J.C. are cofounders of a startup company VivoCor LLC, which is targeting I_{Ks} for the treatment of cardiac arrhythmia. Other authors declare no competing interests.
Received: May 13, 2024. **Accepted:** October 2, 2024
© The Author(s) 2024. Published by Oxford University Press on behalf of National Academy of Sciences. This is an Open Access article distributed under the terms of the Creative Commons Attribution-NonCommercial License (https://creativecommons.org/licenses/by-nc/4.0/), which permits non-commercial re-use, distribution, and reproduction in any medium, provided the original work is properly cited. For commercial re-use, please contact reprints@oup.com for reprints and translation rights for reprints. All other permissions can be obtained through our RightsLink service via the Permissions link on the article page on our site—for further information please contact journals.permissions@oup.com.

which the neurotransmitter norepinephrine (NE) activates the cardiac β-adrenergic receptors, which enhances both inward (e.g. ICa_L, I_F) and outward currents (I_{Ks} and to a much smaller extent I_{Kr}). It achieves these changes by increasing the intracellular cyclic adenosine monophosphate (cAMP) concentration. In the case of I_{Ks}, protein kinase A (PKA) is then activated, and it phosphorylates the I_{Ks} channel (9, 10). The phosphorylation of the channel dramatically increases I_{Ks}, thereby promoting the AP shortening that allows sufficient diastolic refilling during an increase in heart rate (9, 11, 12) (Fig. 1A and B). Clinical studies found that LQT1 patients tend to develop cardiac arrest when the β-adrenergic pathway is activated (for example, when they exercise or are under emotional stress) (9, 12, 13), and LQT1 mutations that impair the β-adrenergic (cAMP) regulation of mutant I_{Ks} channels pose much higher risk of arrhythmia and sudden death to patients than others (14). However, the molecular mechanism underlying the I_{Ks} channel phosphorylation remains elusive, and the lack of means to rescue the defective cAMP response of high-risk variants impedes novel therapeutic options.

KCNQ1, also known as $K_V7.1$, belongs to the classic homotetrameric voltage-gated potassium (K_V) channel subfamily (2–4). Each subunit contains six transmembrane segments (S1–S6), with the S1–S4 forming the voltage-sensing domain (VSD) and the S5–S6 constituting the pore domain (15–18). The VSD activates in response to membrane depolarization in two measurable steps, first to an intermediate (I) state and then to the activated (A) state. Unique to the KCNQ1 channel, the channel pore opens when the VSD is at either I or A state, giving rise to two distinct open states, the intermediate open (IO) and activated open (AO) states (18–24). The coupling between VSD activation and pore opening for the IO and AO states follows a dynamic "hand-and-elbow" gating process, such that movements of S4 in the VSD and subsequent movements of the S4–S5 linker trigger pore opening by interacting with S6 of the same subunit and then with S5 and S6 of a neighboring subunit (22). The IO and AO states have different gating and modulation properties. For example, (i) distinct VSD–pore coupling mechanisms are responsible for the IO and AO states. Multiple LQT1 mutations (e.g. S338F (25)) were found to specifically suppress the VSD–PD coupling of one (AO) state, leaving the mutant channels open only in the other (IO) state (20–22), (ii) KCNQ1 predominantly opens in the IO state, while KCNE1 suppresses the IO state but enhances the AO state, so that the I_{Ks} channel opens only in the AO state (19–23) (Fig. 1C and D), and (iii) a small molecule compound ML277 (26) can increase the AO state current by specifically enhancing the VSD–pore coupling, partially mimicking the KCNE1 function (18, 21, 22).

In this study, we show that the above unique properties of gating and modulation of KCNQ1 are the bases for the mechanism of I_{Ks} channel phosphorylation. Our study uncovers the key role of the KCNQ1 AO state in the channel phosphorylation, and based on these findings, we propose that the AO state from native I_{Ks} channels can be a new target to rescue the defective cAMP sensitivity of high-risk LQT1 mutations. First, using mutagenesis tools that selectively favor the IO and AO states, we found that the AO state of KCNQ1 is responsible for the cAMP response. KCNE1 largely enhances the AO state and therefore boosts the cAMP-induced current increase of KCNQ1. Taking advantage of the unique property that ML277 specifically enhances the AO state, we next found that ML277 can efficiently increase the cAMP sensitivity of both the WT KCNQ1 channel (without KCNE1 association) and the native I_{Ks} channel (with unsaturated KCNE1 association) from guinea pig cardiomyocytes. These results lead to a new strategy for the treatment of lethal LQT1 associated with mutations that impair cAMP sensitivity of I_{Ks}, in which pharmacological reagents can be used to enhance the AO state of the mutant I_{Ks}, thereby recovering the cAMP sensitivity of the mutant channel. To demonstrate this strategy, we studied a high-risk mutation R243C of KCNQ1, which reduced cAMP sensitivity of the I_{Ks} channel, and found that enhancing the AO state occupancy by ML277 rescues the defective cAMP sensitivity of R243C. Taken together, our findings not only reveal the molecular mechanism of the PKA-dependent I_{Ks} phosphorylation but also provide a promising new antiarrhythmic strategy, i.e. to enhance the AO state occupancy of mutant KCNQ1 channels, for high-risk LQT1 variants.

Results

The AO state of KCNQ1 has a higher cAMP sensitivity than the IO state

It is well established that the KCNQ1 channel shows little sensitivity to β-adrenergic stimulation via the cAMP-dependent PKA, but when KCNQ1 is associated with KCNE1, cAMP induces a large current increase (14, 27–30) (Fig. 1A and B). This increase of currents is due to cAMP activation of PKA, which phosphorylates KCNQ1 expressed in oocytes (31, 32) and is consistent with how β-adrenergic stimulation increases I_{Ks} in cardiac myocytes (9, 33) (Fig. S1). The KCNE1-boosted cAMP effect increases the β-adrenergic activation of I_{Ks} to accelerate the repolarization of cardiac APs in adaptation to stress conditions (11, 12, 14, 27–30). However, why the KCNE1 subunit is required for such a cAMP-induced current increase remains unclear. To solve this long-standing puzzle, in this study, we applied membrane permeable cAMP (8-Br-cAMP) to mimic the β-adrenergic stimulation of the KCNQ1 and I_{Ks} channels expressed in *Xenopus* oocytes. We found that 0.5 mM cAMP had a minimum effect on the KCNQ1 current amplitude (19.6 ± 4.8% increase) and the conductance–voltage (G–V) relation but tripled the KCNQ1 + KCNE1 current amplitude (234.3 ± 18.1% increase) and shifted the G–V relation to more negative voltages (Figs. 1B and S2). These results obtained from *Xenopus* oocytes are consistent with findings in mammalian cells such as Chinese hamster ovary cells, Itk^- mouse fibroblast (LM) cells, and human embryonic kidney 293 cells (11, 34, 35).

We then investigated the mechanism for the different cAMP sensitivity in KCNQ1 and I_{Ks} channels. It has been shown that, in response to depolarization, the VSD of KCNQ1 undergoes two steps of activation to the I and A states (19, 20, 22) (Fig. 1C and D). Through a dynamic VSD–pore coupling process, both the I and A state VSD movements induce pore openings; thus, the channel has two different open states, namely IO and AO (18–20, 22) (Fig. 1C and D). The two open states show distinct functional properties including time and voltage dependence, ion permeation, and drug sensitivity (19–22). The KCNQ1 channel primarily opens to the IO state, while KCNE1 suppresses the IO state but enhances the AO state and thus the I_{Ks} channel exclusively opens to the AO state (19, 20, 22, 23).

Based on these previous results, we hypothesize that the IO and AO states have different sensitivities to the cAMP stimulation and the AO state is more sensitive to cAMP than the IO state; thus, the KCNQ1 channel that has primarily the IO state phenotype shows low cAMP sensitivity, while the I_{Ks} channel that has only the AO state phenotype shows enhanced cAMP sensitivity. To test this hypothesis, we utilized our previously identified two pairs of mutant channels that specifically open in the IO or AO state and studied their responses to cAMP stimulation. The first pair, S338F (a long QT syndrome LQT1-associated mutation (25)) and F351A,

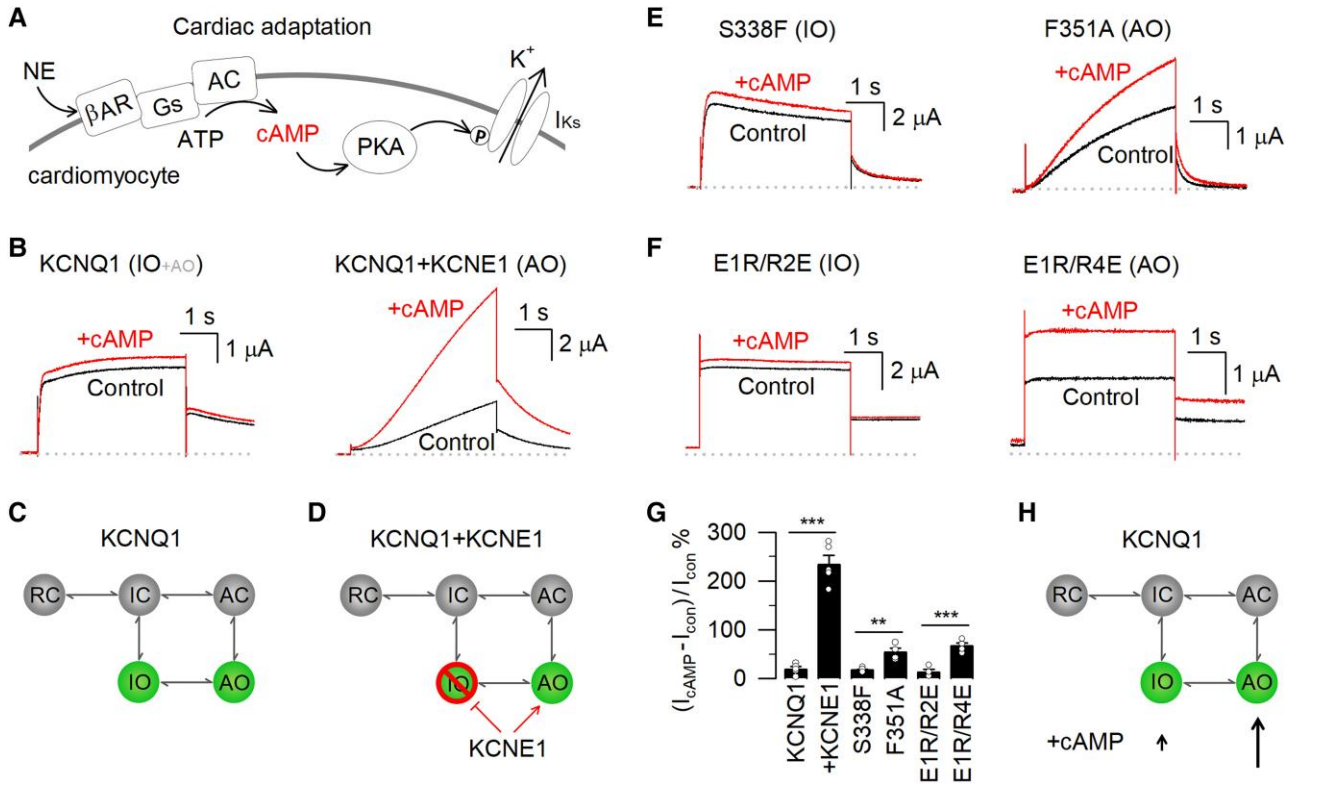

Fig. 1. The AO state of KCNQ1 has higher cAMP sensitivity than the IO state. A) A cartoon model to show the β-adrenergic-dependent up-regulation of I_{Ks} currents in the heart. B) Representative currents of KCNQ1 and KCNQ1 + KCNE1 channels, expressed in *Xenopus* oocytes, before (black) and after (red) adding 0.5 mM cAMP. The test pulse was +40 mV for 4 s. C), D) A cartoon scheme to show the gating mechanism of the KCNQ1 channel. The KCNQ1 channel predominantly opens in the IO state, while KCNE1 suppresses the IO state but enhances the AO state. E), F) Representative currents of S338F and E1R/R2E (open in the IO state) and F351A and E1R/R4E (open in the AO state) before (black) and after (red) adding 0.5 mM cAMP. The test voltage was +40 mV for 4 s and then stepped back to −40 mV. G) cAMP-induced current increases from KCNQ1 alone (19.6 ± 4.8%), KCNQ1 + KCNE1 (234.3 ± 18.1%), S338F (17.6 ± 1.9%), F351A (54.1 ± 8.0%), E1R/R2E (13.7 ± 5.1%), and E1R/R4E (66.6 ± 6.4%). All $n \geq 4$. See Materials and methods for the statistical information. H) A cartoon scheme to illustrate that the AO state is more sensitive to cAMP than the IO state. AC, adenylyl cyclase; Gs, G-protein subunits; NE, norepinephrine; P, phosphate; βAR, β-adrenergic receptor.

selectively disrupt the VSD–pore coupling at the AO and IO states and thus leave the mutant channels open only in the IO and AO states, respectively (20–22). The second pair, E160R/R231E (E1R/R2E) and E160R/R237E (E1R/R4E), arrest the VSD at the I and A states and make the mutant channels constitutively open in the IO and AO states, respectively (19, 20, 22).

We found that the application of 0.5 mM cAMP increased the currents of E1R/R4E and F351A that open in the AO state, but enhanced E1R/R2E or S338F that open to the IO state to a lesser extent (Fig. 1E–G). These results demonstrate that, consistent with our hypothesis, the AO state is more sensitive to cAMP than the IO state (Fig. 1H), which answers the long-standing question of why KCNE1 can boost the cAMP sensitivity of KCNQ1: the association of KCNE1 in I_{Ks} enhances the cAMP-sensitive AO state and suppresses the less cAMP-sensitive IO state, and therefore boosts the cAMP-induced current increase of I_{Ks}.

Increasing the AO occupancy by modulators enhances cAMP sensitivity of KCNQ1

The above results not only show the critical role of the AO state in the KCNQ1 channel cAMP sensitivity, but also suggest that the KCNE1 subunit may not be required for the cAMP-dependent modulation process. Based on this mechanism, we expect that a specific increase of the AO state occupancy in KCNQ1 will enhance its cAMP sensitivity.

We have previously studied the functional effects of the small molecule ML277 on KCNQ1 channels and found that it exclusively enhances the AO state occupancy of the channel. ML277 alters the phenotype of the channel by inducing the AO state with increased current amplitude, a slower activation rate, a right-shifted G–V relation, and a decreased Rb^+/K^+ permeability ratio (21). All these modulations are consistent with the mechanism that ML277 mimics the KCNE1 effects on KCNQ1 to enhance the AO (Fig. 2A). It was demonstrated that ML277 binds to the interface between the VSD and the pore of KCNQ1 (17, 18, 21) and specifically enhances the VSD–pore coupling for the AO state. We therefore tested whether ML277 is capable of increasing cAMP sensitivity of KCNQ1 channels similar to KCNE1. Consistent with our previous results, 1 μM ML277 increased the current amplitude of the slow component without affecting the fast component (Fig. 2B), indicating that the channels opened with an enhanced AO state occupancy (21, 22). Strikingly, in the presence of 1 μM ML277, the KCNQ1 channels were more sensitive to cAMP, such that cAMP-induced larger current increases as compared to KCNQ1 without ML277 (Fig. 2B–E). A higher ML277 concentration (3 μM), which induced a higher AO state occupancy, further boosted the cAMP sensitivity of KCNQ1 (Fig. 2E). We also compared the voltage-dependent activation and found that ML277 and cAMP significantly increased the total maximal conductance, while the G–V relation after adding ML277 and cAMP showed a shift to more positive voltages of ~6 mV (Fig. 2F). This shift was

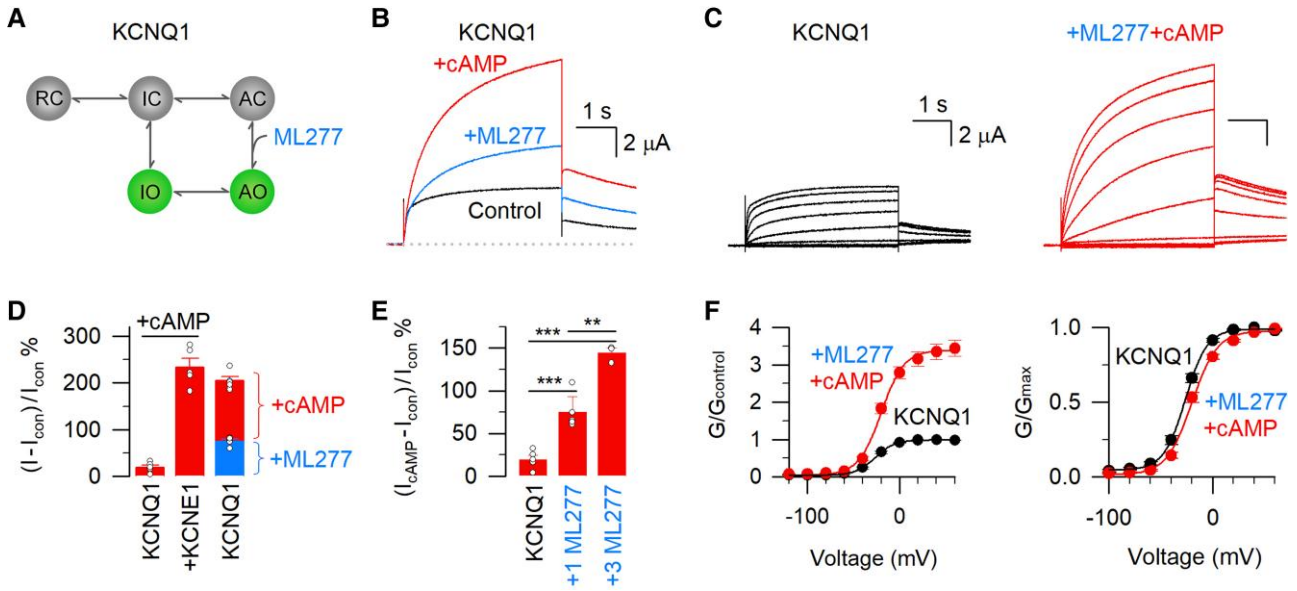

Fig. 2. Increasing AO occupancy by ML277 enhances the cAMP sensitivity of KCNQ1. A) Cartoon schemes to illustrate that ML277 binds at the interface between two neighboring KCNQ1 subunits and specifically enhances the AO state of the KCNQ1 channel, mimicking the KCNE1 effects (21). B) Representative currents of KCNQ1 channel before (black) and after (blue) adding ML277 and then after adding cAMP (red). The test voltage was +40 mV for 4 s and then stepped back to −40 mV. C) Representative activation currents of KCNQ1 before (black) and after (red) adding ML277 and cAMP. D) Current increases of KCNQ1 after adding ML277 (blue, 75.2 ± 4.0%) and cAMP (red, 205.1 ± 8.5%). The same data for cAMP-induced current increases of KCNQ1 (19.6 ± 4.8%) and KCNQ1 + KCNE1 (234.3 ± 18.1%) channels are shown. All $n \geq 4$. E) The cAMP-induced current increases of KCNQ1 before (19.6 ± 4.8%) and after adding 1 μM (74.9 ± 18.1%) and 3 μM (144.2 ± 5.8%) ML277. All $n \geq 3$. F) Left, G–V relations of KCNQ1 before (black) and after (red) adding ML277 and cAMP normalized to control. Right, normalized G–V relations of KCNQ1 before (black) and after (red) adding ML277 and cAMP. All $n \geq 4$.

mainly induced by ML277 due to the increased AO occupancy, which shifted the G–V relation in the direction of the G–V of the AO state as in the I_{Ks} channel (18, 21). These results confirmed the key role of the AO state in modulating the cAMP-dependent phosphorylation of both KCNQ1 and I_{Ks} channels.

To further validate the predominant role of the AO state for cAMP sensitivity, we then proceeded to investigate whether other compounds with the ability to modulate the AO state can likewise enhance the cAMP sensitivity. C28 is a small molecule I_{Ks} activator that was found to bind to the VSD of KCNQ1 (36). Consistent with

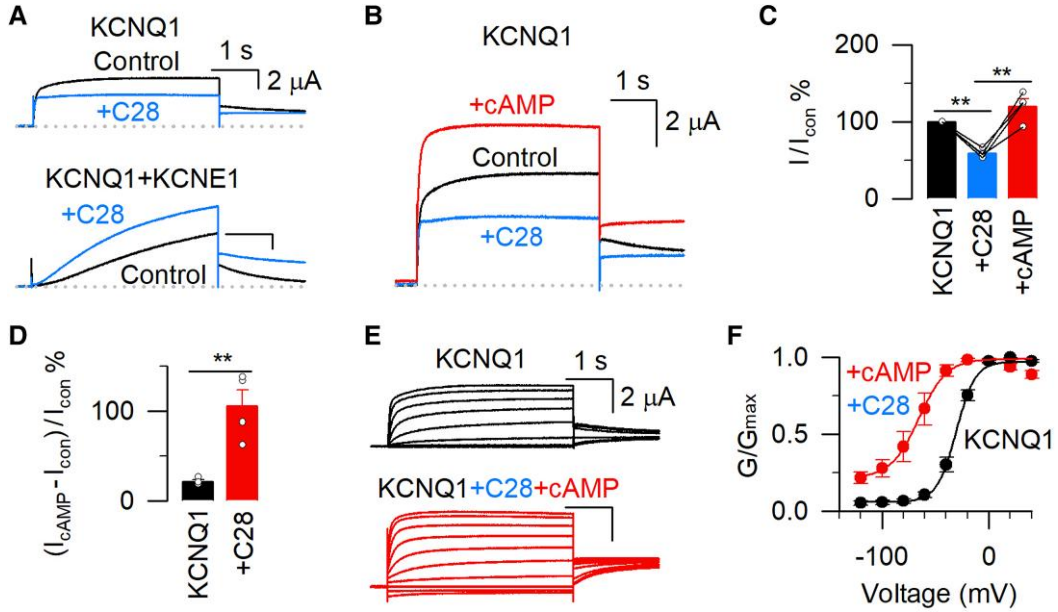

Fig. 3. C28 also boosts the cAMP effects of KCNQ1. A) Representative currents of KCNQ1 and KCNQ1 + KCNE1 before (black) and after (blue) adding 3 μM C28. B) Representative currents of KCNQ1 channel before (black) and after (blue) adding 3 μM C28 and then after adding cAMP (red). C) Normalized current changes of KCNQ1 after adding C28 (blue, from 100% to 58.7 ± 2.9%) and then after adding cAMP (red, from 58.7 ± 2.9% to 119.8 ± 9.6%). D) The cAMP-induced current increases of KCNQ1 (19.6 ± 4.8%) and KCNQ1 after adding C28 (105.3 ± 18.3%). All $n \geq 4$. E) Representative activation currents of KCNQ1 before (black) and after (red) adding C28 and cAMP. F) Normalized G–V relations of KCNQ1 before (black) and after (red) adding C28 and cAMP. All $n \geq 4$.

our previous studies (36), C28 enhanced I_{Ks} but did not enhance the current of KCNQ1 (Fig. 3A). This result was due to C28's preferential enhancement of the AO state occupancy (36). We found in the current study that 3 μM C28 accelerated the activation and slowed down the deactivation of KCNQ1 currents, while it decreased the current amplitude (Fig. 3B and C). These observations are consistent with our previous results (36). Remarkably, after adding C28, 0.5 mM cAMP induced a significantly larger current increase than that of the WT KCNQ1 (105.3 ± 18.3% vs 19.6 ± 4.8%, Fig. 3B–D). We also tested the voltage-dependent activation and found that, after adding C28 and cAMP, the G–V relation of KCNQ1 showed an increased total maximal conductance and a ~35 mV shift to more negative voltages (Fig. 3E and F). This G–V shift was part of the activation effect of C28 (36). Together, these results support that C28, which enhances the AO state occupancy by a different mechanism than ML277, can also sensitize the KCNQ1 channel to cAMP.

ML277 enhances the cAMP sensitivity of native I_{Ks} currents

The β-adrenergic stimulation during physical stresses such as swimming is the main trigger for cardiac events of LQT1 patients, especially in patients whose I_{Ks} lose the cAMP sensitivity, predisposing the patients to high-risk arrhythmias due to compromised cardiac adaptation to stresses (13, 14). The above results suggest that an enhancement of the AO state occupancy can be used as a strategy to increase the response of KCNQ1 to β-adrenergic stimulation in the heart. We next sought to examine this strategy in both native I_{Ks} channels in the heart and mutant I_{Ks} channels that show defective cAMP sensitivity.

Guinea pig ventricular myocytes provide a good model for studying the function of native I_{Ks} currents due to their relatively high expression level of I_{Ks} channels (36–38). In patch clamp whole-cell mode, we injected a 180 pA/10 ms current pulse to induce APs in guinea pig ventricular myocytes at 1 Hz. 10 μM isoproterenol (ISO, a β-adrenergic agonist) was used to mimic the β-adrenergic stimulation in cardiomyocytes. ISO shortened the action potential duration $(APD)_{90}$ and APD_{50}, consistent with the repolarization of cardiac APs being accelerated by increasing the I_{Ks} current after PKA-dependent phosphorylation (Figs. 4A, C, and D and S1D). Interestingly, in the presence of 1 μM ML277, the APs were more sensitive to the ISO stimulation, so that ISO induced increased APD_{90} and APD_{50} shortening as compared to the native I_{Ks} without ML277 (Fig. 4B–D). Of note, ML277 can only activate KCNQ1 but not I_{Ks} with saturated KCNE1 (21, 39). ML277 could modulate the native I_{Ks} in ventricular myocytes because the native I_{Ks} channels are not fully saturated with KCNE1 association (40–44) (see Discussion). These results suggest that in the absence of ML277, ISO mainly works on I_{Ks} channels that are associated with KCNE1; ML277 can boost the cAMP sensitivity of native I_{Ks} channels that are not saturated with KCNE1, so that ISO can modify additional native I_{Ks} channels and, therefore, enhance the APD shortening.

ML277 rescues the defective cAMP effects in the high-risk mutation R243C

The KCNQ1 protein sequence contains 676 amino acids. Among these residues, more than 300 mutations have been found to associate with LQT1, accounting for ~35% of all LQTS cases (7, 8). LQT1 is frequently triggered by adrenergic stimuli, and clinical studies found that the reduced cAMP response and the lethality of LQT1 mutations are associated with the location of the mutations in the channel protein (14, 45). For instance, R243C, a "C-loop" mutation located in the S4–S5 linker (Fig. 5A), reduces the cAMP effect on the mutant I_{Ks} channels and poses a higher risk of arrhythmia and sudden death to patients than other mutations (14). Rescue of the impaired cAMP sensitivity of R243C patients represents a feasible strategy to alleviate the clinical risk under stress conditions.

To achieve this goal, we first characterized the voltage-dependent activation of R243C and R243C-I_{Ks} channels. We found that these channels have similar G–V relations as the WT KCNQ1 and I_{Ks} channels (Fig. 5B). Western blot data in previous studies showed that R243C has a robust membrane expression similar to the WT KCNQ1 (14). However, R243C significantly suppresses KCNE1's effect to boost cAMP sensitivity: the mutant R243C itself shows a low cAMP modulation (21.1 ± 1.9%, Fig. 5C and D), and R243C + KCNE1 also loses most of the cAMP sensitivity as compared to the WT I_{Ks} channel (104.1 ± 8.0%, Fig. 5C and D). These properties suggest that the defective cAMP modulation of R243C-I_{Ks} makes a major contribution to the increased clinical risk of the patients carrying this mutation under stress conditions (14).

Our results in Fig. 1 showed that the KCNE1 subunit boosts the cAMP sensitivity of the I_{Ks} channel by enhancing the AO state of KCNQ1. In the high-risk LQT1 mutation R243C, when the KCNE1's boosting effect is largely reduced, we utilized ML277 as an alternative means to enhance the AO state occupancy of R243C and measured the cAMP effects. Similar to the WT KCNQ1 channel, 1 μM ML277 enhanced the current amplitude by increasing the AO state occupancy (Fig. 6A). We then applied cAMP and measured the current amplitude increase. ML277 clearly boosted the cAMP sensitivity, and thus, the cAMP induced current amplitude more than that of R243C itself (Fig. 6A and B). Furthermore, the G–V relation of R243C after adding ML277 + cAMP also shows a ~9 mV shift to more positive voltages (Fig. 6C). Interestingly, compared with the R243C channel that shows minimum cAMP effect, the same concentration of cAMP induced a greater current increase for R243C + 1 μM ML277 (75.7 ± 7.3%, Fig. 6D and E).

Discussion

In this study, we leverage the unique two open states gating mechanisms of the KCNQ1 channel and the state-dependent mutant channels that selectively open into the IO (S338F and E1R/R2E) and AO (F351A and E1R/R4E) states and find that the AO state is mainly responsible for the cAMP sensitivity of the KCNQ1 and I_{Ks} channels (Fig. 1). This finding answers the long-standing question why the KCNQ1 channel shows only a small current increase, while the I_{Ks} channel shows a large current increase under the β-adrenergic stimulation: KCNQ1 predominantly opens in the IO state so that it shows mainly the less cAMP-sensitive IO state phenotype; the KCNE1 association, on the other hand, suppresses the IO state and enhances the AO state and therefore boosts the cAMP sensitivity of KCNQ1. Taking advantage of the unique feature that small molecules ML277 and C28 can specifically enhance the AO state, we found that they effectively enhance the cAMP sensitivity of the KCNQ1 channel (Figs. 2 and 3). This finding suggests that the cAMP sensitivity of the KCNQ1 channel originates from the AO state of the channel itself, independent of the KCNE1 association, and increasing the AO state occupancy in KCNQ1 may enhance its cAMP sensitivity. These results suggest that enhancing the AO state occupancy of KCNQ1 channels by exogenous modulators can be a new strategy to increase the cAMP sensitivity of native I_{Ks} channels in the heart. We

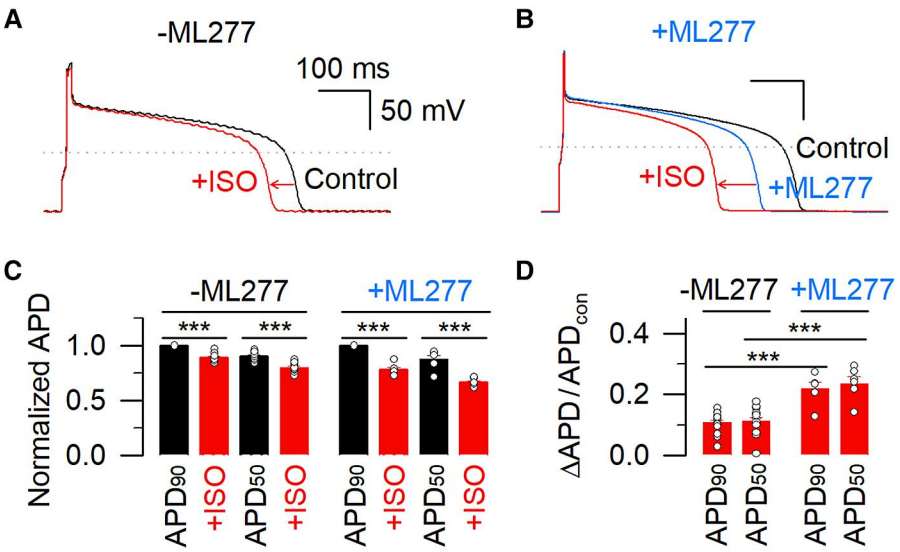

Fig. 4. ML277 increases the cAMP sensitivity of native I_{Ks} currents from guinea pig ventricular myocytes. A) Representative APs of guinea pig ventricular myocytes before (black) and after (red) adding 10 μM ISO. B) Representative APs of guinea pig ventricular myocytes, in the presence of 1 μM ML277, before (blue) and after (red) adding 10 μM ISO. The AP before adding ML277 from the same cell is shown in black. C) Normalized APD. All APD values are normalized to APD_{90} in the absence of ISO. Black, data in the absence of ISO; red, data in the presence of 10 μM ISO. In the absence of ML277, ISO-induced changes were from 1 to 0.89 ± 0.01 for APD_{90} and from 0.91 ± 0.01 to 0.80 ± 0.01 for APD_{50}. In the presence of ML277, ISO-induced changes were from 1 to 0.78 ± 0.02 for APD_{90} and from 0.88 ± 0.04 to 0.67 ± 0.02 for APD_{50}. All $n \geq 6$. D) The ISO-induced changes of APD_{90} and APD_{50}. In the absence of ML277, ISO-induced changes were 0.11 ± 0.01 for APD_{90} and 0.11 ± 0.01 for APD_{50}. In the presence of ML277, ISO-induced changes were 0.22 ± 0.02 for APD_{90} and 0.24 ± 0.02 for APD_{50}. All $n \geq 6$.

confirmed this strategy on native I_{Ks} channels in guinea pig ventricular myocytes and the high-risk LQT1 mutation R243C. ML277 effectively sensitized the cAMP responses of APs from guinea pig ventricular myocytes (Fig. 4) and the high-risk LQT1 mutation R243C (Figs. 5 and 6).

The structure of KCNQ1 shows that the protein adopts two drastically different conformations depending on phosphatidylinositol 4,5-bisphosphate (PIP_2) binding to the VSD (15, 16). In the presence of PIP_2 binding, the S6 transmembrane segment and the cytosolic Helix A form a continuous α-helix such that the cytosolic HelixA–HelixB–CaM (calmodulin) complex shows a distance away from the membrane-spanning domain of the channel, which is known as the cytosolic domain (CTD)-straight conformation (46). In the absence of PIP_2, a loop at the "RQKH" motif downstream of S6 breaks S6 and Helix A into two α-helices with a bend in between. This bend allows the HelixA–HelixB–CaM complex to

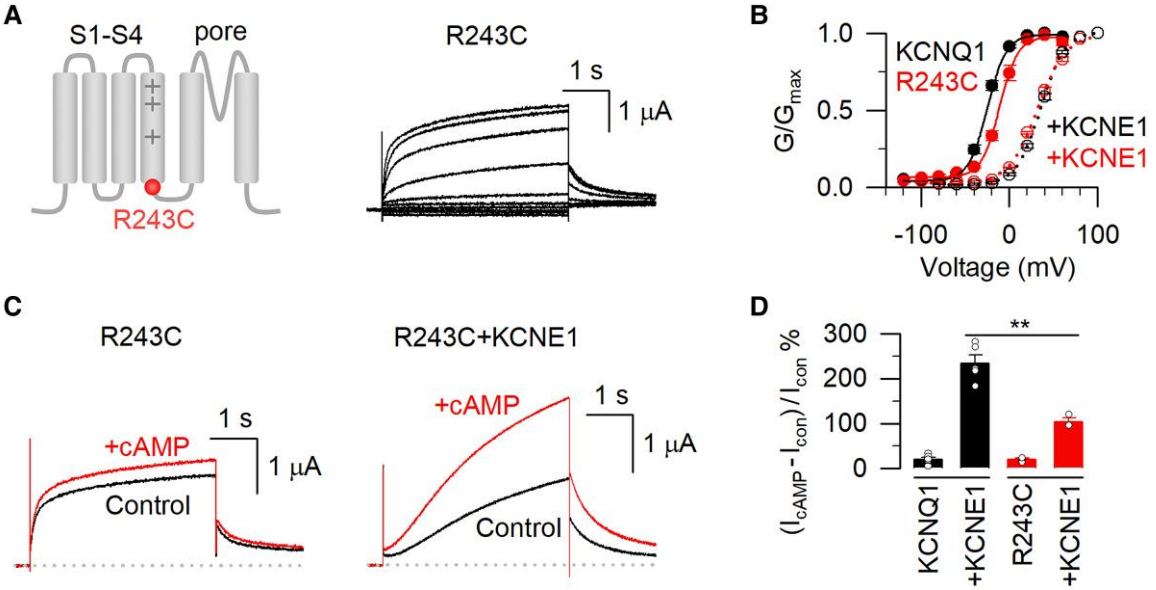

Fig. 5. The high-risk LQT1 mutation R243C + KCNE1 shows impaired cAMP modulation. A) Left, a cartoon of KCNQ1 to show the location of the high-risk LQT1 mutation R243C in the S4–S5 linker. Right, representative currents of R243C elicited by depolarizing voltage pulses (from −120 to +60 mV). B) G–V relations of WT (black) and R243C KCNQ1 (red), with (solid circles) and without (open circles) KCNE1. All $n \geq 4$. C) Representative currents of R243C and R243C + KCNE1 before (black) and after (red) adding 0.5 mM cAMP. D) Average results of cAMP-induced current increase from KCNQ1 (19.6 ± 4.8%), KCNQ1 + KCNE1 (234.3 ± 18.1%), R243C (21.1 ± 1.9%), and R243C + KCNE1 (104.1 ± 8.0%). All $n \geq 3$.

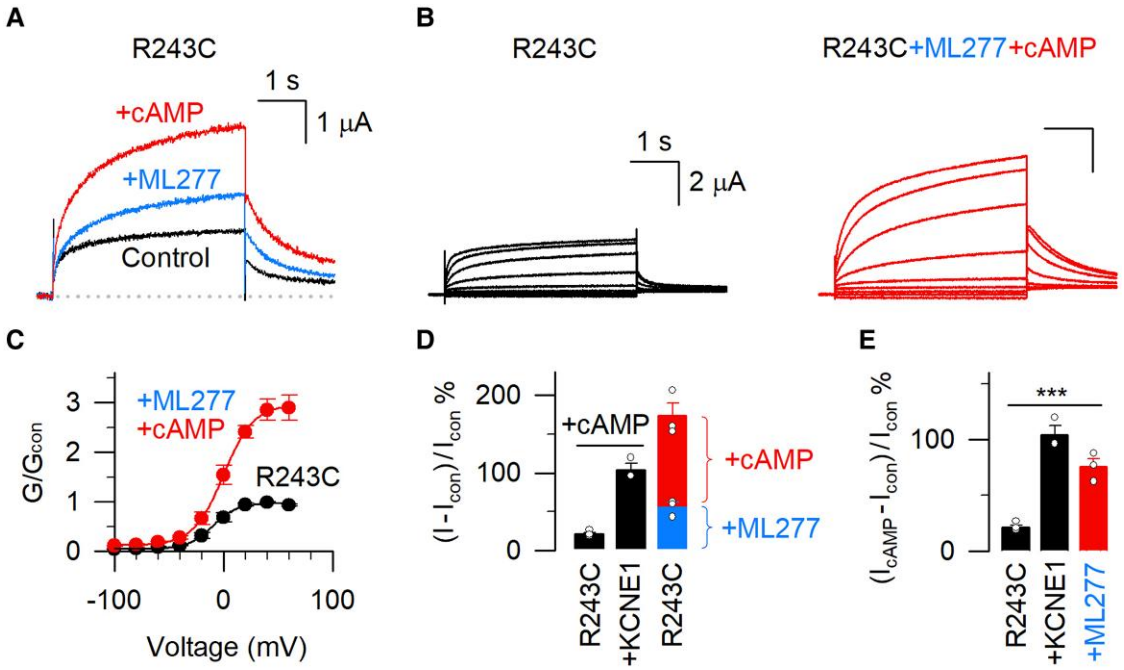

Fig. 6. ML277 rescues the defective cAMP effects in the high-risk mutation R243C. A) Currents of R243C channel before (black) and after (blue) adding ML277 and then after adding cAMP (red). B) Representative activation currents of R243C before (black) and after (red) adding ML277 and cAMP. C) G–V relations of R243C before (black) and after (red) adding ML277 and cAMP. Data are normalized to control. D) Current increases of R243C after adding ML277 (blue, 55.6 ± 6.2%) and cAMP (red, 173.5 ± 16.7%). The cAMP-induced current increases of R243C (21.1 ± 1.9%) and R243C + KCNE1 (104.1 ± 8.0%) channels are shown in black. All $n \geq 4$. E) The cAMP-induced current increases of R243C (21.1 ± 1.9%) and R243C + KCNE1 (104.1 ± 8.0%) and R243C after adding ML277 (75.7 ± 7.3%). The data showed significant differences ("****") by using ANOVA. All $n \geq 3$.

undergo a rotation and translation so that CaM interacts with the linker between the transmembrane segments S2 and S3 (the S2–S3 linker) in the VSD. This conformation is known as the CTD-bent conformation. Our previous study (46) suggested that the IO state corresponds to the CTD-bent conformation, whereas the AO state corresponds to the CTD-straight conformation. PIP_2 binding to the VSD destabilizes the interaction between the S2–S3 linker and CaM to facilitate the transition from IO in the CTD-bent conformation to AO in the CTD-straight conformation. Based on this mechanism, we hypothesize that the PIP_2- and CaM-dependent transition from the CTD-bent to the CTD-straight conformation alters the effects of PKA phosphorylation on channel activation; thus, the AO state is more sensitive to cAMP application.

The cAMP-dependent modulation of the I_{Ks} channel plays a key role in the cardiac adaptation under stress conditions. For LQT1 patients, β-adrenergic stimulation is the main trigger for cardiac events. LQT1 mutations that reduce cAMP sensitivity of the mutant I_{Ks} currents show a higher risk of cardiac events and increased lethality (13, 14). However, so far, no strategy has been reported to rescue this defective cAMP modulation. Our findings in this study clearly show that enhancing the AO state occupancy of KCNQ1 channels can be a new antiarrhythmic strategy, especially for the high-risk variants where the KCNE1's effect of boosting cAMP sensitivity is largely suppressed.

Interestingly, several lines of evidence have demonstrated that in native I_{Ks} currents, KCNQ1 can associate with KCNE1 at various stoichiometries. First, in vitro stoichiometry studies show that one tetrameric KCNQ1 channel can associate with different numbers of KCNE1 (from 0 to 4), depending on the KCNQ1/KCNE1 expression ratio (40–42, 44, 47–49). Second, in vivo studies in ventricular myocytes suggest that the ratio of KCNQ1/KCNE1 does not remain stable but changes dynamically in different conditions over time and pathology progression (43, 50–52). Third, the G–V relations of native I_{Ks} currents from neonatal mouse, guinea pig, and rabbit ventricular myocytes fall in between that of the KCNQ1 only and I_{Ks} with saturated KCNE1 association (37, 53). Fourth, although ML277 selectively activates the KCNQ1 channel but not the I_{Ks} channel with saturated KCNE1 association, pharmacological studies in guinea pig ventricular myocytes, human induced pluripotent stem cell-derived cardiomyocytes, and zebrafish hearts show that ML277 effectively shortens the APD via activating native I_{Ks} currents (Fig. 4) (39, 54, 55). These results consistently suggest that in cardiomyocytes, the native I_{Ks} channels are not fully saturated with KCNE1 association. The KCNQ1 subunits not associated with KCNE1 constitute the "KCNQ1 component" in native I_{Ks} channels that can be further modulated by small molecules such as ML277. Consistent with this finding, the Fedida lab has quantified the cAMP effects on I_{Ks} channels with different KCNQ1/KCNE1 stoichiometries, and they found that cAMP induces no V_{50} shift on the WT KCNQ1 channel, but gradually increases with the number of KCNE1 binding to the I_{Ks} channel (35). These results indicate that our proposed antiarrhythmic strategy of boosting cAMP sensitivity of native and mutant I_{Ks} by increasing the AO state of the channel using exogenous modulators can be effective in treating LQT1 patients.

Materials and methods

Constructs and mutagenesis

Overlap extension and high-fidelity PCR were used for making KCNQ1 channel point mutations. Each KCNQ1 mutation was verified by DNA sequencing. Then, cRNA of WT and mutant

KCNQ1 was synthesized using the mMessage T7 polymerase kit (Applied Biosystems–Thermo Fisher Scientific) for oocyte injections.

Oocyte preparation and channel expression

Oocytes (at stage V or VI) were obtained from *Xenopus laevis* by laparotomy. All procedures are consistent with the recommendations of the Panel on Euthanasia of the American Veterinary Medical Association. Oocytes were digested by collagenase (0.5 mg/mL, Sigma-Aldrich) and micro-injected with KCNQ1 and KCNE1 cRNAs. WT or mutant KCNQ1 cRNAs (9.2 ng) with or without KCNE1 cRNA were injected into each oocyte with a KCNQ1/KCNE1 weight ratio of 4:1, which could saturate the KCNE1 association to KCNQ1 (21, 41). Injected cells were kept in ND96 solution (in mM): 96 NaCl, 2 KCl, 1.8 $CaCl_2$, 1 $MgCl_2$, 5 HEPES, 2.5 CH_3COCO_2Na, 1:100 Pen-Strep, pH 7.6, at 18 °C for 2–6 days for electrophysiology recordings.

Two-electrode voltage clamp

Microelectrodes (Sutter Instrument, item no. B150-117-10) were made with a Sutter (P-97) puller with 1–3 MΩ resistances when filled with 3 M KCl. The extracellular solution was ND96 solution without CH_3COCO_2Na. Currents were recorded with a CA-1B amplifier (Dagan, Minneapolis, MN, USA) with Patchmaster (HEKA) software. Signals were sampled at 1 kHz and low-pass-filtered at 2 kHz. ML277 and cAMP stocks (Sigma-Aldrich) were added to the bath and diluted to working concentrations. All recordings were performed at room temperature (21–23 °C). Data were analyzed with Clampfit (Axon Instruments, Inc., Sunnyvale, CA, USA), Sigmaplot (SPSS, Inc., San Jose, CA, USA), and IGOR (Wavemetrics, Lake Oswego, OR, USA). The membrane permeable PKA inhibitor 14–22 amide (Sigma-Aldrich, 476485) was added to the incubation solution ND96 (100 nM) for oocytes after injection of KCNQ1 + KCNE1 mRNA. The currents and cAMP effects were measured after 2 days.

Endogenous Yotiao detection by RT-PCR

The A-kinase-anchoring protein (AKAP, also named Yotiao) is required for the PKA-dependent phosphorylation of the I_{Ks} channel (9). We found that in *Xenopus* oocytes, the I_{Ks} channel without human Yotiao (h-Yotiao) injection is activated by cAMP to a similar extent to that after h-Yotiao injection (KCNQ1/h-Yotiao mRNA weight ratio was 1:1), which suggests that there is endogenous frog Yotiao (f-Yotiao) in *Xenopus* oocytes that has similar function to the h-Yotiao (Fig. S3).

To confirm the existence of endogenous f-Yotiao in *Xenopus* oocytes, total RNAs were extracted from 30 h-Yotiao injected or uninjected *Xenopus* Oocytes. Experiments were carried out using a Purelink RNA extract mini kit (Thermo Fisher Scientific, USA). Subsequently, the isolated RNA was converted to cDNA using an iScript cDNA Synthesis Kit (Bio-Rad, USA). The PCR was conducted using Herculase II Fusion DNA Polymerase (Agilent, USA). The sequences of both f- and h-Yotiao were acquired from the National Center for Biotechnology Information. The oligonucleotide forward primer sequence used for both f- and h-Yotiao is GAGCAGCTGAGTTCTGAGA. The reverse primer sequences were GGCCGAGACTGTCCAGTA for h-Yotiao and CTGTGTGAATCAGACTGTTC for f-Yotiao. The amplified DNA fragments for the human F–R primer pair have a length of 557 bp, while the amplified DNA fragments for the frog F–R primer pair have a length of 563 bp (Fig. S3). The endogenous f-Yotiao protein was found to have a similar function to the h-Yotiao in the PKA-dependent phosphorylation of the I_{Ks} channel (Fig. S3). Therefore, we did not inject h-Yotiao in other experiments with oocytes.

Guinea pig cardiomyocytes preparation and AP recording

Cardiac myocyte isolation: The use of guinea pigs was approved by the Stony Brook University Institutional Animal Care and Use Committee. Single ventricular myocytes were acutely enzymatically isolated from guinea pig heart as previously described (56). Guinea pigs, weighing 300–500 g, were sacrificed by peritoneal injection of sodium pentobarbitone (1 mL, 390 mg/mL). The isolated cells were stored in the solution containing (in mM) 83 KCl, 30 K_2HPO_4, 5 $MgSO_4$, 5 Na-pyruvate, 5 β-OH-butyric acid, 20 creatine, 20 taurine, 10 glucose, 0.5 EGTA, pH 7.2. Electrophysiological recording of APs: APs were recorded with whole-cell current clamp recording. Freshly isolated guinea pig cardiac myocytes were paced at 1 Hz with a 180 pA pulse current for 10 ms duration to generate APs. The APD_{90} and APD_{50} were determined at 90 and 50% repolarization from the peak amplitude, respectively. Several minutes were allowed for the APD to reach steady state before data were collected. The extracellular solution contains (in mM): 140 NaCl, 3 KCl, 1 $MgCl_2$, 1.8 $CaCl_2$, 10 HEPES, 10 glucose, pH 7.4. The pipette solution contains (in mM): 115 K-aspartic acid, 35 KOH, 3 $MgCl_2$, 10 HEPES, 11 EGTA, 5 glucose, 3 MgATP, pH 7.4. All recordings were performed at room temperature (21–23 °C).

Statistical analysis

All averaged data were collected from at least three different cells. Data were presented as mean ± SEM, with "*n*" indicating the number of independent experiments. Differences between two groups exhibiting normal distribution were analyzed using the t test or paired t test, and differences among more than two groups were analyzed using one-way ANOVA. Statistical analyses were conducted using Sigmaplot. Statistical significance was established at $^{*}P < 0.05$, $^{**}P < 0.01$, and $^{***}P < 0.001$.

Acknowledgments

This work was supported by NIH grants RO1 HL126774, HL155398, and US–Israel Binational Science Foundation research grant 2019159 to J.C.; HL166628 to I.S.C. and AHA postdoctoral fellowship 18POST34030203 to P.H. P.H. was also supported by the following grants in writing the manuscript: National Natural Science Foundation of China (32171221) and Macau Science and Technology Development Fund (0074/2022/A2 and 0098/2023/RIA2).

Supplementary Material

Supplementary material is available at *PNAS Nexus* online.

Funding

NIH grants: RO1 HL126774, RO1 HL155398 (J.C.) US-Israel Binational Science Foundation Research Grant 2019159 (J.C.) NIH grants: RO1 HL166628 (I.S.C.) AHA postdoctoral fellowship 18POST34030203 (P.H.) National Natural Science Foundation of China 32171221 (P.H.) Macau Science and Technology Development Fund 0074/2022/A2 and 0098/2023/RIA2 (P.H.).

Author Contributions

P.H. and J.C: conceptualization; I.S.C. and J.C.: supervision; P.H., L.Z., L.Zhong., J.S., H.Z.W., J.G., H.C., and J.Z: data curation; P.H., I.S.C., and J.C.: formal analysis; P.H. and J.C.: writing-original draft; and all authors: writing-review and editing.

Preprint

This manuscript was posted on a preprint: https://biorxiv.org/cgi/content/short/2024.07.02.601749v1.

Data Availability

All study data are included in the article and/or supporting information.

References

1 Nerbonne JM, Kass RS. 2005. Molecular physiology of cardiac repolarization. *Physiol Rev*. 85(4):1205–1253.
2 Wang Q, *et al*. 1996. Positional cloning of a novel potassium channel gene: KVLQT1 mutations cause cardiac arrhythmias. *Nat Genet*. 12(1):17–23.
3 Sanguinetti MC, *et al*. 1996. Coassembly of K(V)LQT1 and minK (IsK) proteins to form cardiac I(Ks) potassium channel. *Nature*. 384(6604):80–83.
4 Roden DM. 2004. Drug-induced prolongation of the QT interval. *N Engl J Med*. 350(10):1013–1022.
5 Barhanin J, *et al*. 1996. K(V)LQT1 and lsK (minK) proteins associate to form the I(Ks) cardiac potassium current. *Nature*. 384(6604):78–80.
6 Tester DJ, Ackerman MJ. 2014. Genetics of long QT syndrome. *Methodist Debakey Cardiovasc J*. 10(1):29–33.
7 Ackerman MJ, *et al*. 2011. HRS/EHRA expert consensus statement on the state of genetic testing for the channelopathies and cardiomyopathies: this document was developed as a partnership between the Heart Rhythm Society (HRS) and the European Heart Rhythm Association (EHRA). *Europace*. 13(8):1077–1109.
8 Bohnen MS, *et al*. 2017. Molecular pathophysiology of congenital long QT syndrome. *Physiol Rev*. 97(1):89–134.
9 Marx SO, *et al*. 2002. Requirement of a macromolecular signaling complex for beta adrenergic receptor modulation of the KCNQ1-KCNE1 potassium channel. *Science*. 295(5554):496–499.
10 Chen L, Kurokawa J, Kass RS. 2005. Phosphorylation of the A-kinase-anchoring protein Yotiao contributes to protein kinase A regulation of a heart potassium channel. *J Biol Chem*. 280(36):31347–31352.
11 Kurokawa J, Chen L, Kass RS. 2003. Requirement of subunit expression for cAMP-mediated regulation of a heart potassium channel. *Proc Natl Acad Sci U S A*. 100(4):2122–2127.
12 Terrenoire C, Clancy CE, Cormier JW, Sampson KJ, Kass RS. 2005. Autonomic control of cardiac action potentials: role of potassium channel kinetics in response to sympathetic stimulation. *Circ Res*. 96(5):e25–e34.
13 Schwartz PJ, Volders PG. 2014. Sudden death by stress: how far under the nerves should we dig to find out why LQT1 patients die? *J Am Coll Cardiol*. 63(8):828–830.
14 Barsheshet A, *et al*. 2012. Mutations in cytoplasmic loops of the KCNQ1 channel and the risk of life-threatening events: implications for mutation-specific response to beta-blocker therapy in type 1 long-QT syndrome. *Circulation*. 125(16):1988–1996.
15 Sun J, MacKinnon R. 2017. Cryo-EM structure of a KCNQ1/CaM complex reveals insights into congenital long QT syndrome. *Cell*. 169(6):1042–1050.e9.
16 Sun J, MacKinnon R. 2020. Structural basis of human KCNQ1 modulation and gating. *Cell*. 180(2):340–347 e349.
17 Willegems K, *et al*. 2022. Structural and electrophysiological basis for the modulation of KCNQ1 channel currents by ML277. *Nat Commun*. 13(1):3760.
18 Ma D, *et al*. 2022. Structural mechanisms for the activation of human cardiac KCNQ1 channel by electro-mechanical coupling enhancers. *Proc Natl Acad Sci U S A*. 119(45):e2207067119.
19 Zaydman MA, *et al*. 2014. Domain-domain interactions determine the gating, permeation, pharmacology, and subunit modulation of the IKs ion channel. *eLife*. 3:e03606.
20 Hou P, *et al*. 2017. Inactivation of KCNQ1 potassium channels reveals dynamic coupling between voltage sensing and pore opening. *Nat Commun*. 8(1):1730.
21 Hou P, Shi J, White KM, Gao Y, Cui J. 2019. ML277 specifically enhances the fully activated open state of KCNQ1 by modulating VSD-pore coupling. *eLife*. 8:e48576.
22 Hou P, *et al*. 2020. Two-stage electro-mechanical coupling of a KV channel in voltage-dependent activation. *Nat Commun*. 11(1):676.
23 Taylor KC, *et al*. 2020. Structure and physiological function of the human KCNQ1 channel voltage sensor intermediate state. *eLife*. 9:e53901.
24 Barro-Soria R, *et al*. 2017. KCNE1 and KCNE3 modulate KCNQ1 channels by affecting different gating transitions. *Proc Natl Acad Sci U S A*. 114(35):E7367–E7376.
25 Hoosien M, *et al*. 2013. Dysfunctional potassium channel subunit interaction as a novel mechanism of long QT syndrome. *Heart rhythm*. 10(5):728–737.
26 Mattmann ME, *et al*. 2012. Identification of (R)-N-(4-(4-methoxyphenyl)thiazol-2-yl)-1-tosylpiperidine-2-carboxamide, ML277, as a novel, potent and selective K(v)7.1 (KCNQ1) potassium channel activator. *Bioorg Med Chem Lett*. 22(18):5936–5941.
27 Brink PA, *et al*. 2005. Phenotypic variability and unusual clinical severity of congenital long-QT syndrome in a founder population. *Circulation*. 112(17):2602–2610.
28 Crotti L, *et al*. 2007. The common long-QT syndrome mutation KCNQ1/A341 V causes unusually severe clinical manifestations in patients with different ethnic backgrounds: toward a mutation-specific risk stratification. *Circulation*. 116(21):2366–2375.
29 Heijman J, *et al*. 2012. Dominant-negative control of cAMP-dependent IKs upregulation in human long-QT syndrome type 1. *Circ Res*. 110(2):211–219.
30 Schwartz PJ, *et al*. 2001. Genotype-phenotype correlation in the long-QT syndrome: gene-specific triggers for life-threatening arrhythmias. *Circulation*. 103(1):89–95.
31 Blumenthal EM, Kaczmarek LK. 1992. Modulation by cAMP of a slowly activating potassium channel expressed in *Xenopus* oocytes. *J Neurosci*. 12(l):290–296.
32 Kurokawa J, Motoike HK, Rao J, Kass RS. 2004. Regulatory actions of the A-kinase anchoring protein Yotiao on a heart potassium channel downstream of PKA phosphorylation. *Proc Natl Acad Sci U S A*. 101(46):16374–16378.
33 Harmati G, *et al*. 2011. Effects of β-adrenoceptor stimulation on delayed rectifier K^+ currents in canine ventricular cardiomyocytes. *Br J Pharmacol*. 162:890–896.
34 Thompson E, *et al*. 2017. cAMP-dependent regulation of IKs single-channel kinetics. *J Gen Physiol*. 149(8):781–798.

35 Thompson E, Eldstrom J, Westhoff M, McAfee D, Fedida D. 2018. The I(Ks) channel response to cAMP is modulated by the KCNE1: KCNQ1 stoichiometry. *Biophys J*. 115(9):1731–1740.

36 Lin Y, *et al*. 2021. Modulating the voltage sensor of a cardiac potassium channel shows antiarrhythmic effects. *Proc Natl Acad Sci U S A*. 118(20):e2024215118.

37 Lu Z, Kamiya K, Opthof T, Yasui K, Kodama I. 2001. Density and kinetics of I(Kr) and I(Ks) in guinea pig and rabbit ventricular myocytes explain different efficacy of I(Ks) blockade at high heart rate in guinea pig and rabbit: implications for arrhythmogenesis in humans. *Circulation*. 104(8):951–956.

38 Lu Z, *et al*. 2012. Suppression of phosphoinositide 3-kinase signaling and alteration of multiple ion currents in drug-induced long QT syndrome. *Sci Transl Med*. 4(131):131ra150.

39 Yu H, *et al*. 2013. Dynamic subunit stoichiometry confers a progressive continuum of pharmacological sensitivity by KCNQ potassium channels. *Proc Natl Acad Sci U S A*. 110(21):8732–8737.

40 Chen H, Kim LA, Rajan S, Xu S, Goldstein SA. 2003. Charybdotoxin binding in the I(Ks) pore demonstrates two MinK subunits in each channel complex. *Neuron*. 40(1):15–23.

41 Nakajo K, Ulbrich MH, Kubo Y, Isacoff EY. 2010. Stoichiometry of the KCNQ1—KCNE1 ion channel complex. *Proc Natl Acad Sci U S A*. 107(44):18862–18867.

42 Murray CI, *et al*. 2016. Unnatural amino acid photo-crosslinking of the IKs channel complex demonstrates a KCNE1:KCNQ1 stoichiometry of up to 4:4. *eLife*. 5:e11815.

43 Jiang M, Wang Y, Tseng GN. 2017. Adult ventricular myocytes segregate KCNQ1 and KCNE1 to keep the IKs amplitude in check until when larger IKs is needed. *Circ Arrhythm Electrophysiol*. 10(6): e005084.

44 Morin TJ, Kobertz WR. 2008. Counting membrane-embedded KCNE beta- subunits in functioning K+ channel complexes. *Proc Natl Acad Sci U S A*. 105(5):1478–1482.

45 Schwartz PJ, *et al*. 2021. Mutation location and IKs regulation in the arrhythmic risk of long QT syndrome type 1: the importance of the KCNQ1 S6 region. *Eur Heart J*. 42(46):4743–4755.

46 Kang PW, *et al*. 2020. Calmodulin acts as a state-dependent switch to control a cardiac potassium channel opening. *Sci Adv*. 6(50):eabd6798.

47 Wang W, Xia J, Kass RS. 1998. MinK-KvLQT1 fusion proteins, evidence for multiple stoichiometries of the assembled IsK channel. *J Biol Chem*. 273(51):34069–34074.

48 Westhoff M, Eldstrom J, Murray CI, Thompson E, Fedida D. 2019. I Ks ion- channel pore conductance can result from individual voltage sensor movements. *Proc Natl Acad Sci U S A*. 116(16): 7879–7888.

49 Cui J, Kline RP, Pennefather P, Cohen IS. 1994. Gating of IsK expressed in *Xenopus* oocytes depends on the amount of mRNA injected. *J Gen Physiol*. 104(1):87–105.

50 Oliveras A, *et al*. 2020. The unconventional biogenesis of Kv7.1-KCNE1 complexes. *Sci Adv*. 6(14):eaay4472.

51 Aflaki M, *et al*. 2014. Exchange protein directly activated by cAMP mediates slow delayed-rectifier current remodeling by sustained beta-adrenergic activation in guinea pig hearts. *Circ Res*. 114(6): 993–1003.

52 Xu Parks X, Qudsi H, Braun C, Lopes CMB. 2020. The auxiliary subunit KCNE1 regulates KCNQ1 channel response to sustained calcium-dependent PKC activation. *PLoS One*. 15(8):e0237591.

53 Xiong D, *et al*. 2017. SUMOylation determines the voltage required to activate cardiac I(Ks) channels. *Proc Natl Acad Sci U S A*. 114(32):E6686–E6694.

54 Xu Y, *et al*. 2015. Probing binding sites and mechanisms of action of an I(Ks) activator by computations and experiments. *Biophys J*. 108(1):62–75.

55 De la Cruz A, *et al*. 2023. Pharmacological screening of Kv7.1 and Kv7.1/KCNE1 activators as potential antiarrhythmic drugs in the zebrafish heart. *Int J Mol Sci*. 24(15):12092.

56 Gao J, Mathias RT, Cohen IS, Baldo GJ. 1992. Isoprenaline, Ca^{2+} and the Na(+)-K+ pump in guinea-pig ventricular myocytes. *J Physiol*. 449:689–704.